https://doi.org/10.31925/farmacia.2024.6.21 **ORIGINAL ARTICLE**

DEVELOPMENT AND CHARACTERISATION OF IMPLANTABLE SANDWICH STRUCTURES MADE OF LITHIUM-DOPED BIOLOGICAL-DERIVED HYDROXYAPATITE AND CIPROFLOXACIN

OANA ANDREEA ZUREIGAT [1], JOHNY NEAMȚU [1], LIVIU DUTA [2]*, MĂDĂLINA ICRIVERZI [3], PAULA FLORIAN [3], LIVIA-ELENA SIMA [3], GABRIELA DORCIOMAN [2], VALENTINA GRUMEZESCU [2], ROXANA-MARIA BĂLĂȘOIU [1], SANDRA ALICE BUTEICĂ [1], RENATA MARIA VĂRUȚ [1], OANA ELENA NICOLAESCU [1]

[1]*University of Medicine and Pharmacy, Faculty of Pharmacy, 2 Petru Rareş Str., 200349 Craiova, Dolj County, Romania*
[2]*National Institute for Laser, Plasma and Radiation Physics, 409 Atomiştilor Str., 077125 Măgurele, Romania*
[3]*Institute of Biochemistry of the Romanian Academy, 296 Spl. Independenței, 060031 Bucharest, Romania*

**corresponding author: liviu.duta@inflpr.ro*

Manuscript received: October 2024

Abstract

To address the limitations of synthetic hydroxyapatite (HA), which lacks the precise chemical composition of natural bone minerals, alternative, cost-effective production methods from sustainable biological resources, termed BioHA, have been investigated. Incorporating CIP into BioHA-based implant coatings enables localised, high-concentration antibiotic release directly at infection sites, thereby reducing systemic exposure and associated side effects. In this study, we utilised Matrix-Assisted Pulsed Laser Evaporation (MAPLE) for the deposition of CIP, achieving sustained concentrations above the minimum inhibitory concentration for *Staphylococcus aureus* throughout a 21-day release period. Biocompatibility assays revealed that hMSCs adhered to titanium (Ti) surfaces with CIP-loaded coatings exhibited significantly reduced proliferation rates compared to control Ti surfaces. Moreover, indirect cytotoxicity assessments indicated that, while no significant cytotoxic effects were induced on any of the surfaces, a modest reduction in hMSC proliferation was observed in the presence of CIP. These findings highlight the complex interplay between antimicrobial agents and stem cell behaviour, underscoring the necessity for careful consideration in designing biomaterials for clinical applications.

Rezumat

Pentru a aborda limitările hidroxiapatitei sintetice (HA) care nu are compoziția chimică exactă a mineralelor osoase naturale, au fost explorate metode de producție rentabile ca și alternative, din surse biologice durabile, BioHA. Includerea CIPei (CIP) în implanturile pe bază de BioHA permite eliberarea de antibiotice localizată, într-o concentrație mare la situsul infecției, evitând expunerea sistemică și minimizând potențialele efecte secundare ale antibioticului. În studiul nostru, care a folosit tehnica MAPLE pentru depunerea CIP, s-au menținut concentrațiile CIP peste concentrația minimă inhibitorie (MIC) pentru Staphylococcus aureus pe tot parcursul studiului de eliberare, cu profiluri de eliberare susținută extinse până la 21 de zile. Experimentele de biocompatibilitate au indicat că hMSC-urile aderate la suprafețele de Ti cu acoperiri încărcate cu CIPă au prezentat rate de proliferare semnificativ mai mici în comparație cu suprafețele de control Ti. În plus, testele indirecte de citotoxicitate au arătat că, în timp ce toate suprafețele analizate nu au indus efecte citotoxice semnificative, a fost observată o ușoară scădere a proliferării hMSC în prezența CIPei. Aceste constatări subliniază interacțiunile complexe dintre agenții antimicrobieni și comportamentul celulelor stem, subliniind necesitatea unei analize atente în proiectarea biomaterialelor pentru aplicații clinice.

Keywords: CIP, titanium implants, antibacterial activity, biocompatibility, sandwich structures, PLD/MAPLE techniques

Introduction

Recent studies have underscored the therapeutic potential of biomaterials, demonstrating their efficacy as a viable treatment strategy [32, 42]. The rise in life expectancy and a higher incidence of injuries and disease have notably increased the demand for dental and orthopaedic devices. In response, the functionalisation of implant surfaces with advanced bioactive materials has emerged as a crucial approach to minimise implant failures and extend their functional lifespan [22].

Titanium (Ti) bone implants are medical devices extensively used in orthopaedic and dental surgery to replace or repair damaged bone tissue and to support existing bone structures. Ti is a widely used metal in medical applications due to its remarkable properties, including high biocompatibility, excellent corrosion resistance and substantial durability. As a biocompatible material, Ti is well tolerated by human tissues. It has a low propensity to induce allergic reactions or immunological rejection [52], making it an ideal candidate for long-term implantation in the body.

While beneficial in many applications, HA implants can present limitations in specific surgical contexts. Specifically, they may be less suited for regions subjected to high mechanical stress or patients requiring more resilient materials. Due to their inherent brittleness, HA implants require particularly cautious handling during surgery to prevent damage or fractures [6]. Furthermore, successful implantation of HA-based materials demands precise preparation and technique, necessitating specialists in orthopaedics or dentistry to conduct these procedures to ensure optimal outcomes [26].

In this context, additive manufacturing (AM) is a technology that enables the rapid and cost-effective production of complex three-dimensional (3D) metal parts, and it is currently gaining increased attention in the field of personalised medicine [31, 12]. Despite their excellent mechanical properties, Ti implants exhibit relatively low osseointegration rates. To overcome this drawback, HA can be applied as a surface coating on Ti implants, thereby enhancing their overall performance by merging the superior bioactivity of ceramics with the mechanical resilience of metallic substrates [21]. Further optimisation of these properties is being explored by doping HA with therapeutic ions or antibiotics to increase osseointegration and provide antimicrobial protection [18, 23, 44]. Effective implant coatings must fulfil stringent criteria, including biocompatibility, non-toxicity and osseointegrative capacity. Typically, these coatings are added as a supplementary layer on the implant's surface without compromising the intrinsic properties of the underlying material. This can be achieved through various techniques, such as electrochemical deposition [29], sol-gel processing [38], pulsed laser deposition (PLD) and matrix-assisted pulsed laser evaporation (MAPLE).

PLD is a thin film synthesis technique consisting of the ablation by a focused, high-power, pulsed laser beam of a solid target in a vacuum environment and the condensation of the resulting vapour phase on a deposition substrate placed parallel to the holder [14, 28, 43]. In contrast, MAPLE is a versatile and efficient technique widely used for depositing thin films of organic materials, such as pharmaceuticals, polymers and biomolecules. Originally derived from conventional PLD, the MAPLE method enables the gentle deposition of fragile organic molecules, preserving their functional and structural integrity. In the MAPLE process, the material of interest is dissolved in a volatile solvent and then frozen to form a solid target. This frozen target is irradiated by a pulsed laser, usually in the ultraviolet (UV) range [10, 11, 24, 15]. The solvent matrix absorbs the laser energy, causing localised heating and evaporation of solvent and solute molecules. Due to the differential volatility between the solvent and the organic molecules, the solvent evaporates rapidly. In contrast, the organic molecules are deposited as a thin film on a substrate parallel to the target. One of the major advantages of MAPLE is its ability to deposit high-quality thin films of complex organic compounds without causing thermal or photochemical degradation. This is particularly relevant for sensitive materials like ciprofloxacin (CIP), an antibiotic used in various medical applications. Traditional deposition techniques often face challenges with such molecules because of their susceptibility to breakdown under high-energy conditions. In contrast, MAPLE minimises molecular fragmentation, allowing the functional properties of CIP to be preserved in the deposited thin film, which is crucial for applications requiring precise control over biological activity and drug release.

Implant materials are often treated with antibacterial agents *via* diverse surface modification techniques to improve osseointegration and mitigate infection risks. Current strategies are directed at developing Ti implant coatings that facilitate the controlled release of antibacterial agents [3].

Incorporating CIP into bone cement is advantageous for high-risk patients undergoing joint replacement surgeries, where infection prevention is paramount for successful outcomes. Its application in antibiotic-loaded systems has been associated with notably lower infection rates than conventional, non-antibiotic-loaded controls.

This work aims to contribute to developing high-performance sandwich structures - BioHA doped with lithium phosphate (further denoted as BioHA: LiP) and CIP - functionalised onto medical grade Ti implants using both PLD and MAPLE techniques. These implant coatings, alongside their established benefits of low manufacturing costs, accessibility and sustainable resource utilisation, are engineered to enhance mechanical properties, antimicrobial efficiency and biocompatibility.

Materials and Methods

Powder preparation

The BioHA powders were obtained from bovine femoral bones purchased on the market. Before usage, they were submitted to veterinary control. The bones were cut into small pieces and washed with distilled water. They were then introduced for two weeks in an alkaline sodium hypochlorite solution (1%) for deproteinization. It should be emphasised here that the 1% concentration of sodium hypochlorite is widely used in the literature to effectively remove organic material from biological precursors without excessive degradation of the calcium content or contamination from residual reagents. This concentration strikes a balance between ensuring the complete removal of organic content and maintaining the structural integrity of the precursor material [14, 15, 28, 38]. After washing and drying, all the bone pieces were calcined at 850°C for 4 h in the air (Protherm oven, Alserteknik Inc., Istanbul, Turkey) to eliminate organic bone components. The calcination protocol was selected based on prior

studies and experimental validation. A temperature of 850°C was chosen to ensure the complete removal of organic residues without significant sintering or phase transformation, whilst 4 h was determined as sufficient for achieving a uniform and complete conversion of the biological material [14, 15, 28, 38]. The as-prepared bone pieces were crushed by grinding and introduced into a ball mill to obtain fine powders. Finally, all powders were calcined using a similar protocol, with a heating rate of 4°C/min. The preparation of BioHA powders was in accordance with the EU settlement No. 722/2012 and ISO No. 22442-1:2015. LiP powder (LOT # MKBD3219V, code: 338893 - 100G, Sigma Aldrich, St. Louis, MI, USA) was incorporated into BioHA in a concentration of 1 wt.%. Batches of BioHA:LiP of approximately 40 g were prepared by powder mechanical mixing using a high-energy Retsch S 100 ball mill in an open-air environment (milling duration of approximately 15 min, at 200 rot/min). Fine powders (*i.e.*, with particles of submicron mean size) were thus obtained [15].

Targets preparation

Approximately 2.5 g of BioHA:LiP powder mixtures were introduced into a stainless-steel mould (Specac Ltd., Orpington, UK) with a diameter of 2 cm. The mixed powders were next compacted by pressing at approximately 6 MPa. This compaction pressure was selected to achieve sufficient green density for the compacted hydroxyapatite powder while avoiding excessive particle crushing or tool wear. No lubricants or compaction aids were used in this process to maintain material purity [14, 15, 38]. Pellets with a thickness of 0.5 cm were thus obtained. Next, the pellets were sintered at 700°C for 4 h (heating rate 5°C/min, natural cooling down) and further used as targets for the PLD experiments.

CIP (Sigma Aldrich, St. Louis, MI, USA) powder was suspended in 10 mL of deionised water. The solution was mixed in an Erlenmeyer glass, which was continuously stirred. Four mL was poured into a Cu cup (diameter 30 mm, height 5 mm), frozen at liquid nitrogen temperature (77 K), and used as a target for MAPLE experiments. The experimental setup is depicted schematically in Figure 1.

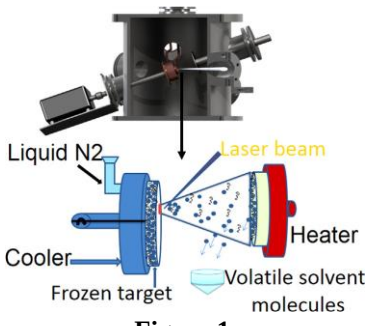

Figure 1.
MAPLE experimental set-up. Reproduced from Reference [51], with permission from Elsevier

PLD/MAPLE sandwich structures

All experiments were performed inside a stainless-steel deposition chamber, using a pulsed UV KrF* COMPexPro 205F excimer laser source ($\lambda = 248$ nm, $\tau_{FWHM} \leq 25$ ns) (Coherent, Santa Clara, CA, USA), operated at a frequency repetition rate of 10 Hz (PLD) and 13 Hz (MAPLE). The depositions were performed using a two-step procedure: first, one set of samples (*i.e.*, BioHA and BioHA:LiP) was synthesised by PLD technique, while a second one was fabricated using MAPLE method by deposition of CIP (1 wt.%) on top of PLD thin films (*i.e.*, BioHA:LiP-CIP - sandwich structures).

The ablated material was transferred and collected both onto medical-grade Ti substrates (φ = 12 mm, thickness 1.5 mm) and double-side polished Si (100) wafers of (1 × 1) cm^2 (Medapteh Plus Cert SRL, Măgurele, Romania). They were placed parallel to the target surface at a separation distance of approximately 5 cm. Before introduction inside the deposition chamber, all substrates were cleaned in an ultrasonic bath Elmasonic X-tra 30H (Elma Schmidbauer GmbH, Singen, Germany), according to a laboratory protocol previously described [18].

The laser beam was incident at 45° onto the target's surface, and the fluence was set at 4 J/cm^2 (PLD) and 300 mJ/cm^2 (MAPLE). To ensure a top-hat laser spot and the repeatability of the samples, a dedicated beam homogeniser (single-axis type) was used in all MAPLE experiments.

During PLD depositions, all substrates were heated and maintained at a constant temperature of 500°C by a PID-Excel temperature controller (Excel Instruments, Mumbai, India). The heating and cooling ramps were 20 and 10°C/min, respectively. All MAPLE experiments were carried out at room temperature (RT).

To avoid piercing and possible modification of the surface morphology induced by the laser radiation, both PLD and MAPLE targets were continuously rotated during the multi-pulse deposition process with a frequency of 0.83 Hz (50 rot/min). For the deposition of one coating, 15,000 (PLD) and 100,000 (MAPLE) consecutive laser pulses were applied.

The PLD experiments were performed in water vapour-enriched ambient at a residual pressure of 3.75×10^{-1} Torr (~ 50 Pa), while MAPLE depositions were done at a pressure of approximately 2.3×10^{-4} mbar.

Post-deposition thermal treatments

The as-deposited PLD coatings were subjected to post-deposition thermal treatments for 6 hours at the same temperature used during the dispositions (500°C) in a water-vapour ambient.

Characterisation of PLD/MAPLE synthesised sandwich structures

Adsorption of CIP. The BioHA:LiP-CIP weighed implant coatings were wholly immersed in a CIP solution (0.3 mg CIP *per* 10 mL of ultrapure water) for 48 hours. After immersion, they were placed on

filter paper, allowed to dry at RT for an additional 48 hours and subsequently weighed.

FTIR analysis. Fourier transform infrared (FTIR) spectroscopy investigated the coatings' chemical structure. An IRTracer-100 equipment (Shimadzu), operated in an attenuated total reflectance (ATR) mode with a diamond head (0.18 cm diameter), was used. All measurements were performed at RT, in the range (1600 - 500) cm^{-1}, with a resolution of 4 cm^{-1} and a total number of 64 scans/experiment.

CIP determination in the release medium. High-performance liquid chromatography (HPLC) analysis was conducted using a Vanquish Core LC system with a manual injector, coupled with a Diode Array Detector (DAD) from Thermo Fisher Scientific (USA), and data acquisition management through Chromeleon 7 software. Separation was performed on a C18 reverse-phase column (Thermo Scientific, Acclaim™ 120), measuring 100 mm in length and 4.6 mm in inner diameter, with a stationary phase particle size of 5 µm. The mobile phase comprised a citrate buffer solution at pH = 3.1 (16.7 mM citric acid dihydrate and 3.3 mM sodium citrate dihydrate) and acetonitrile in a 70:30 (v/v) ratio, with a flow rate set at 1 mL/min. All experiments were conducted at RT.

A 1 mg/mL CIP stock solution was prepared in citrate buffer, followed by ultrasonication and storage at 4°C. Subsequently, serial dilution with citrate buffer prepared working solutions ranging from 0.125 µg/mL to 20 µg/mL.

In vitro release studies. In vitro release studies were conducted on CIP adsorbed on the surface of BioHA:LiP Ti discs abbreviated BioHA:LiP-CIP (Adsorption) and deposited through MAPLE on the surface of BioHA:LiP Ti discs abbreviated BioHA:LiP-CIP (MAPLE). The temperature was controlled in an incubator at 37 ± 0.5°C. Virals with threaded caps were used to maintain airtight conditions during measurements. Initially, 10 mL of HPLC-grade ultrapure water (Li-Chrosolv, Merck) was added, and the BioHA:LiP-CIP (Adsorption) and BioHA:LiP-CIP (MAPLE) samples were immersed. At specific time intervals (1 h, 6 h, 12 h, 24 h, 48 h, 72 h, 96 h, 5 days, 7 days, 8 days, 10 days, 11 days and 14 days), 0.5 mL of the solution was collected for quantitative analysis of CIP release *via* HPLC. The extracted volume was replaced with ultrapure water to prevent CIP saturation in the medium. From each collected sample, 20 µL was injected into the HPLC system for analysis [8].

Biocompatibility tests. Human mesenchymal stem cells (hMSCs) were isolated by plate adherence from bone marrow collected from the femoral diaphysis of a patient with total hip arthroplasty [35, 45]. The cells were cultured in Dulbecco's Minimal Essential Medium GlutaMAX® with low glucose content (1 g/L), supplemented with 10% FBS (v/v, heat-inactivated) and 1% penicillin-streptomycin (PE/ST), then were and maintained in culture in 175 cm^2 flasks at a density of 1.0×10^6 cells *per* flask at 37°C in an incubator with a 5% CO_2 atmosphere. Cell viability was assessed using 0.4% Trypan Blue reagent. Experiments were conducted with cells with viability more significant than 95% and at passages 14 - 16. The tested materials were sterilised by UV treatment for 15 minutes in a Thermo Safe hood before all biological assays.

hMSCs were seeded at a density of 5000 cells/cm^2 in 24-well culture plates and incubated for 72 hours in a humidified atmosphere with 5% CO_2 at 37°C, allowing direct contact with the surfaces of the studied materials. Cell viability was quantitatively assessed after 72 hours using a colorimetric method using the MTS assay (CellTiter 96® Aqueous One Solution Proliferation Assay kit, Promega). This essay measured cell viability on the material surfaces and in the culture medium in contact with the tested materials, providing insights into surface interaction and potential leachate effects on cell health.

The assay relies on dehydrogenase enzymes present in metabolically active cells, reducing the reagent to formazan, with the quantity of formazan produced directly correlating to the number of viable cells. Following a 2-hour incubation at 37°C with the MTS reagent (at a 1:5 dilution in a pre-warmed complete medium) in the absence of light, 100 µL of the resulting supernatant was transferred to a 96-well microplate. The optical density was subsequently measured at 450 nm using a Mithras Berthold micro-plate reader, facilitating quantitative analysis of cell viability.

Antibacterial activity

Preparation of culture medium and bacterial inoculation. Mueller-Hinton nutrient agar was dispensed into 100 mm diameter Petri dishes to form a uniform 4 mm layer. The bacterial inoculum was prepared by suspending 2 - 3 standard colonies in physiological saline, with the turbidity adjusted nephelometrically to ensure consistency. The medium, with a pH of 7.3, was formulated to support optimal bacterial growth for the species under investigation. Inoculation involved flooding the agar surface with the bacterial suspension and carefully removing excess liquid. The inoculated plates were then allowed to dry at RT for 10 minutes before sample application.

The microorganisms tested were standard reference strains sourced from the Cantacuzino Institute and verified as susceptible to the selected antibiotic, CIP.

CIP minimum inhibitory concentration. To determine the MIC, filter paper discs impregnated with varying concentrations of CIP (2, 3, 4, 5, 6, 7 and 8 µg) were placed on culture media previously inoculated with *S. aureus*. The Petri dishes were then incubated at 37°C for 24 hours for bacterial growth and antibiotic interaction.

Antibiogram. The antibacterial effect was assessed using the diffusion method on nutrient agar, following the Kirby-Bauer protocol by FR X standards. Test

discs were positioned 1.5 cm from the edge of the Petri dish and spaced 3 cm apart to prevent overlapping diffusion zones. The plates were incubated in an inverted position at 37°C for 18 hours for optimal diffusion and bacterial interaction.

The results were assessed visually, with a graduated ruler used to measure the diameter of the inhibition zones (in mm) produced by the test samples. Data were reported as mean values, calculated by determining the arithmetic average of the inhibition zone diameters measured across three replicates.

The diameters of the inhibition zones measured for the test samples were compared with the standard inhibition diameter of the reference antibiotic and the control diameter (absence of treatment, denoted as "-"). Observations of very small colonies, secondary invasion within the inhibition zone, or slight growth inside the inhibition area were disregarded in the analysis. As this method is qualitative, it does not allow for direct quantification of antibacterial activity but provides a comparative measure of efficacy based on inhibition zone sizes.

Statistical Analysis

All experiments were conducted in triplicate (n = 3) to ensure statistical significance. The significance level was determined using Student's t-test, with p-values of ≤ 0.05 considered statistically significant and p-values of ≤ 0.0001 and ≤ 0.00001 denoting high and very high significance, respectively. Statistical analysis for biocompatibility tests was performed with GraphPad Prism 6 software (GraphPad, San Diego, CA, USA) using one-way ANOVA with Tukey's multiple comparison tests.

Results and Discussion

FT-IR investigations

FTIR spectroscopy obtained absorption bands to characterise CIP and confirm its molecular structure (Figure 2). Absorption bands in the 1300 - 1390 cm^{-1} region correspond to C-N stretching vibrations [41], characteristic of secondary amines present in CIP. C-F stretching vibrations were also detected between 1035 and 1100 cm^{-1}, further supporting the structural identification [27].

It should also be noted that the bands observed between 630 and 650 cm^{-1} represent the symmetric stretching vibrations of phosphate groups in BioHA:LiP films [1]. Peaks in the 1030 - 1090 cm^{-1} region are attributed to the asymmetric stretching vibrations of the PO_4^{3-} groups, indicative of the phosphate structures within these compounds.

In vitro release studies

A calibration curve was generated, yielding the equation y = 3.7496x + 0.4234, where y represents the peak surface area (mAu·min) and x denotes the concentration of CIP in µg/mL (Figure 3). This linear relationship facilitates the quantification of CIP concentration in samples based on measured peak surface areas.

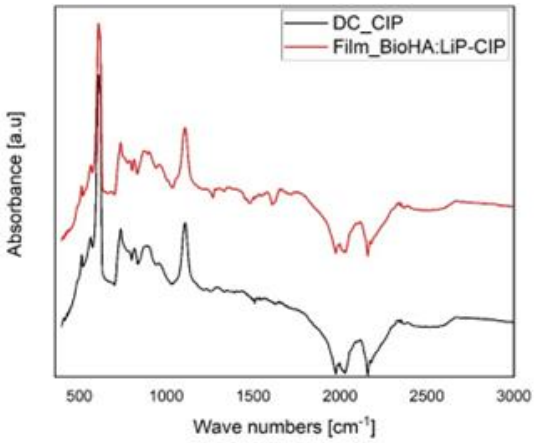

Figure 2.
FTIR spectra of CIP (red line - BioHA:LiP-CIP thin film synthesized by PLD/MAPLE; black line - CIP drop cast)

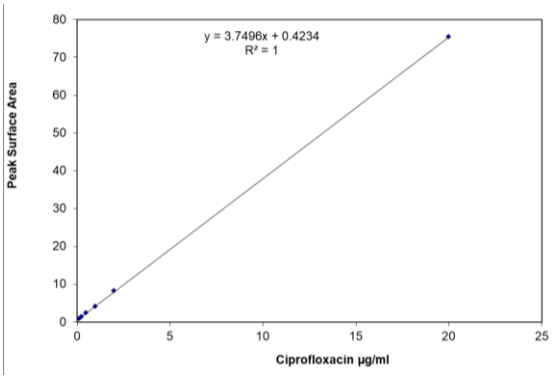

Figure 3.
The calibration curve was obtained for CIP using the HPLC-DAD method

The release profile of CIP varied significantly with experimental conditions. An initial burst release was observed from the BioHA:LiP-CIP (Adsorption) formulation, with a substantial amount of CIP released within the first 6 hours of the experiment (Figure 5). This was followed by a slower, sustained release phase. By day 10, the amount of CIP released had decreased to a very low level, falling below the MIC of 0.6 µg/mL. The release of CIP from the BioHA:LiP-CIP (MAPLE) system persisted over 14 days, exhibiting a sustained release profile with CIP concentrations consistently maintained above the MIC value, as illustrated in Figure 4 and Figure 5. This continuous release indicates a controlled release mechanism that may enhance the formulation's therapeutic efficacy.

Antibacterial activity

The MIC was defined as the lowest concentration of antibiotic required to inhibit visible bacterial growth *in vitro*, as presented in Table I.

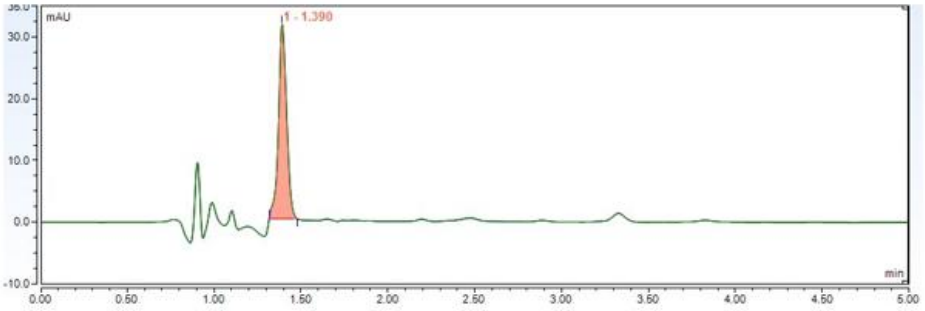

A

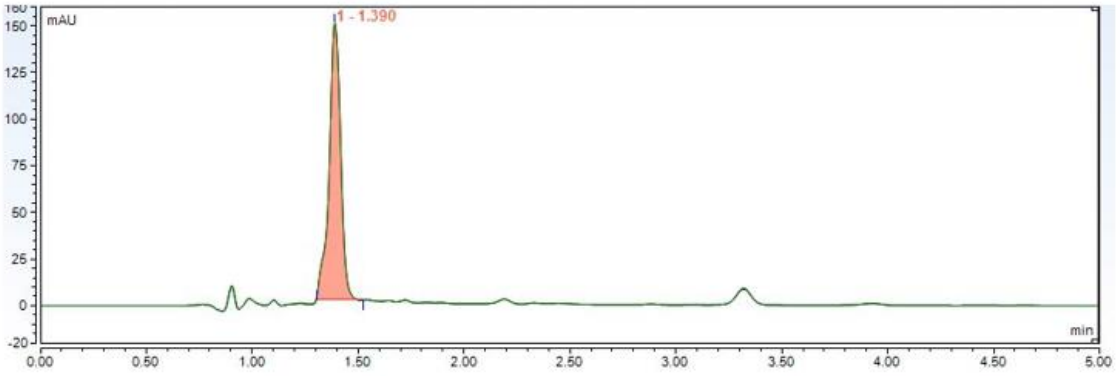

B

Figure 4.

Chromatograms obtained for CIP release from:
(A) BioHA:LiP-CIP (Adsorbtion) at 10 days; (B) BioHA:LiP-CIP (MAPLE) at 1 hour

Table I

Classification of sensitivity of tested strains to CIP based on inhibition zone diameter

Microorganism test	R (mm)	IS (mm)	S (mm)
Staphylococcus aureus	≤ 14	16 - 20	≥ 21

Results are reported as follows: S (sensitive), IS (intermediate-sensitive) and R (resistant), according to the diameter of the inhibition zone in the bacterial culture.

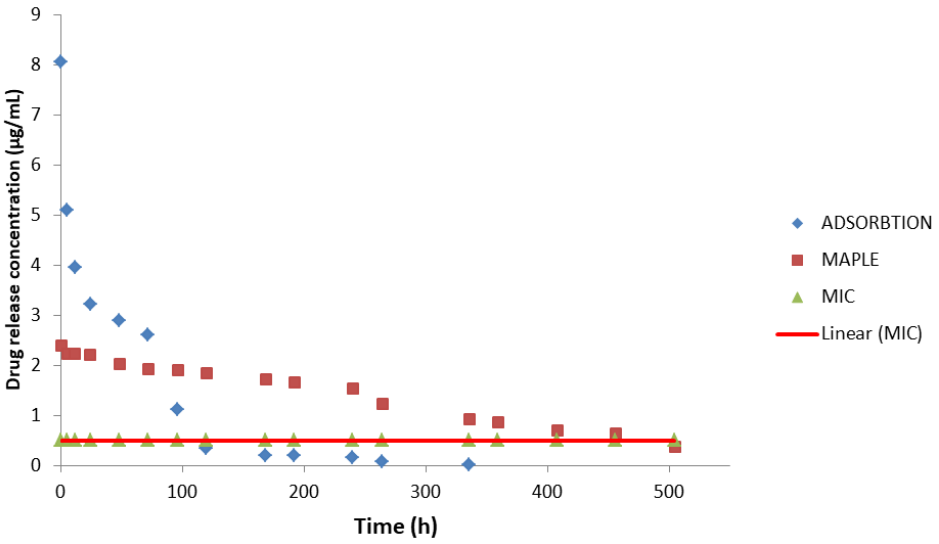

Figure 5.

CIP release concentration over time

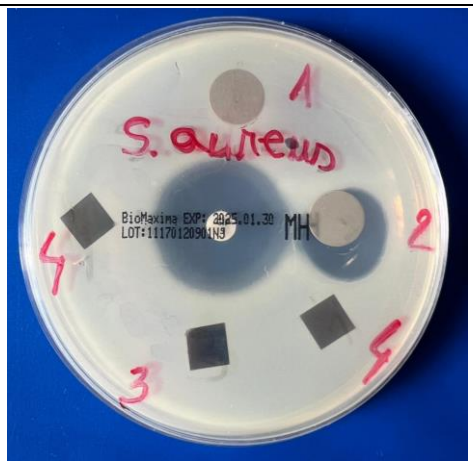

Figure 6.
Inhibition zones observed for (1) BioHA; (2) BioHA:LiP-CIP (MAPLE); (3) BioHA:LiP; (4) uncoated Ti (control) and CIP standard (centre) on *Staphylococcus aureus via* disk diffusion agar method

Table II categorises the average inhibition zone diameters (DZI, in mm) based on bacterial sensitivity. The values reflect the mean diameters of inhibition zones, providing a quantitative measure of bacterial growth inhibition for each tested condition.

As Figure 6 and Table II demonstrated, the BioHA:LiP-CIP (MAPLE) sandwich structure exhibited antibacterial activity, evidenced by an inhibition zone with a diameter of 20 mm. This indicates that the sample can be classified as intermediate-sensitive relative to the CIP standard, which showed a larger inhibition zone of 29 mm. The reduced inhibition zone diameter is likely due to its significantly lower CIP concentration than the standard formulation.

Biocompatibility tests

Biocompatibility tests involving direct (Figure 7a) and indirect (Figure 7b) contact with hMSC cells were performed. Cells were seeded on the material surfaces, and their viability and proliferation were assessed after 72 hours using the MTS assay. As shown in Figure 7, results indicate significant differences in cell adhesion and proliferation among the coated surfaces. hMSCs adhered to Ti surfaces with various coatings (BioHA, BioHA:LiP and BioHA:LiP-CIP (MAPLE)) demonstrated reduced proliferation compared to the control cells grown on uncoated (control) Ti, showing an approximate 50% reduction in proliferation. Notably, the BioHA:LiP-CIP (MAPLE) surfaces exhibited a marked decrease in metabolic activity, with over an 80% reduction, indicating a significant impact of this coating on cell viability and proliferation.

Table II

Average diameters of bacterial growth inhibition zones (*resistant, **intermediate, ***sensitive)

Test product	DZI *Staphylococcus aureus*
CPX (5 µg)	29 ***
Uncoated Ti (control)	0 *
BioHA:LiP	0 *
BioHA:LiP-CIP (Adsorption)	28.7 ***
BioHA:LiP-CIP (MAPLE)	20 **

DZI stands for the average value of inhibition zone diameters (mm).

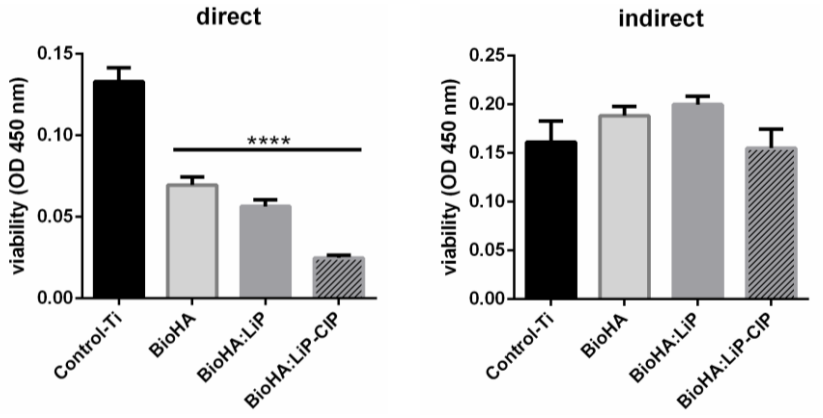

(a) (b)

Figure 7.
Viability of hMSC cells after 72 hours: (a) grown directly on the tested surfaces (Control-Ti, BioHA, BioHA:LiP and BioHA:LiP-CIP (direct contact assays); and (b) exposed to the medium in which the tested surfaces were incubated (indirect contact assays)
Results are shown as mean ± standard deviation values of triplicates in each group. ****$p < 0.0001$ *vs.* Control-Ti.

Additionally, *in vitro* tests were conducted to assess the indirect cytotoxic effects of coated and uncoated Ti discs on hMSC cells. In these experiments, hMSCs adhered to the culture plate and were exposed to the

conditioned medium where the materials had been incubated for 72 hours. This setup allowed for the evaluation of potential cytotoxic effects exerted by leachable or degradation products from the materials on the adhered hMSC cells.

In the indirect cytotoxicity assessment (Figure 7b), it was observed that none of the analysed surfaces, regardless of coating type, induced a cytotoxic effect, as evidenced by continued hMSC proliferation. However, a slight reduction in proliferation was noted in hMSC cells exposed to the medium from uncoated Ti surfaces and coverslips. This indicates that while the BioHA:LiP-CIP (MAPLE) coating does not exhibit overt cytotoxicity, it may slightly influence cell proliferation relative to uncoated controls.

Ti is an exceptionally strong metal, rendering it highly suitable for bone structures that endure mechanical forces and pressures. Ti implants are engineered to withstand routine wear and physical stress, making them ideal for diverse surgical applications, such as joint replacement, bone fracture reinforcement and dental implants [48, 49]. These implants can be tailored into various shapes and sizes to accommodate the specific anatomical and functional requirements of individual patients. As a radiopaque material, Ti can be readily visualised in medical imaging modalities, including X-rays and CT scans, facilitating effective monitoring and assessment of implant integrity and progress.

Hydroxyapatite (HA) is a naturally occurring mineral compound in human bone, renowned for its compatibility with bone tissue [34]. Due to its structural similarity to native bone minerals, HA is highly suitable for incorporation into bone implants. These implants are used in various orthopaedic and dental applications [13], addressing conditions such as bone fractures, and bone loss due to disease or injury and providing support for dental implants [47]. Synthetic HA is typically produced through complex chemical procedures. An alternative, sustainable approach to obtaining natural HA involves extracting it from abundant biological resources, such as bones derived from the food-processing industry [40]. Animal bone-derived HA (referred to as BioHA) has been shown to contain various trace elements (*e.g.*, Na, Mg, Sr and K), each with specific bio-functional roles, which distinguishes it from synthetic HA. Furthermore, BioHA exhibits enhanced mechanical properties and a more dynamic environmental response [16].

Infection risk associated with implant materials remains critical in orthopaedic practice and warrants careful attention. Infections surrounding implant materials pose a significant complication in orthopaedic surgeries. When an infection develops near an implant, it may lead to surgical failure and prolonged recovery times for patients. While antibiotics are a standard treatment, their potential side effects necessitate cautious consideration. Additionally, bacterial colonisation of implanted materials can result in biofilm formation, which markedly reduces the efficacy of bactericidal treatments.

Staphylococcus aureus, a Gram-positive bacteria, is a well-researched pathogen implicated in bone infections. This bacterium can form multicellular biofilms, which serve as protective barriers against host immune responses. Furthermore, *S. aureus* has evolved diverse defence mechanisms, with its biofilms exhibiting notably enhanced resistance to antibiotic treatment.

CIP is a selective antibiotic in bone implants because of its potent antimicrobial properties and capacity to sustain high localised concentrations at the implantation site. This targeted delivery enhances its efficacy in preventing infections associated with orthopaedic implants.

CIP exhibits a broad spectrum of activity, effectively targeting various bacterial strains, particularly Gram-negative and select Gram-positive organisms [9]. This broad-spectrum efficacy makes CIP a valuable agent for preventing and managing infections that may arise post-surgically, especially in orthopaedic procedures where the risk of infection is notably high. Its use in this context helps mitigate potential postoperative complications, supporting improved patient outcomes in orthopaedic care.

The minimum inhibitory concentration (MIC) of CIP varies significantly, ranging from as low as 0.25 μg/mL in susceptible bacterial strains to over 256 μg/mL in resistant strains, depending on the specific bacterial species and their resistance profiles [37]. CIP demonstrates high bioavailability and has proven effective in penetrating bone tissues, enabling it to achieve therapeutic levels within bone – a crucial property for treating localised infections [20].

To address the limitation that synthetic HA does not fully replicate the chemical composition of natural bone minerals [49], considerable efforts have been directed toward developing alternative, cost-effective methods for HA production, such as sourcing it from sustainable, biological resources, including biogenic mammalian or fish bones (BioHA). BioHA is a carbonate-containing, non-stoichiometric, calcium-deficient material that significantly differs from synthetic HA in composition, stoichiometry, crystal size and morphology, crystallinity, degradation rate and overall biological performance [30]. These distinctions can enhance the biological compatibility and functionality of BioHA materials in bone-related applications.

A key factor driving increased interest in BioHA is the presence of trace elements and functional groups that modify the chemical formula of natural bone-derived HA. Unlike chemically synthesised HA, which lacks these components, mammalian bones provide a rich source of ions and trace elements [17], with Na^+ and Mg^{2+} being the most common. When present with HA, these ions play a crucial role in bone and tooth development, as their absence can lead to bone fragility or loss [12].

In vitro release studies

S. aureus is frequently isolated in osteomyelitis cases and is a common pathogen responsible for bone infections. It can cause significant bone destruction and is often associated with chronic infections due to its biofilm-forming capability, which complicates treatment [33]. CIP treats infections caused by *S. aureus*, including methicillin-sensitive (MSSA) and methicillin-resistant (MRSA) strains. For MRSA, the MIC of CIP has been reported to be as low as 0.5 μg/mL [7].

Incorporating CIP into HA-based implant coatings allows for localised release, achieving high antibiotic concentrations directly at the infection site while minimising systemic exposure. This targeted delivery approach reduces the risk of systemic side effects associated with higher antibiotic doses. Studies have demonstrated that CIP-loaded implant coatings can attain elevated local concentrations, essential for effectively managing bacterial infections such as osteomyelitis [39]. In our research, CIP deposition *via* MAPLE ensured sustained concentrations above the MIC (μg/mL) for clinical isolates of *S. aureus* [19] throughout the entire *in vitro* release period, lasting up to 21 days.

Biocompatibility tests

The biocompatibility of CIP about hMSCs is influenced by its antimicrobial properties, which, while effective against bacterial cells, can adversely impact cell viability and proliferation in mammalian cells. CIP's mechanism of action involves inhibiting DNA gyrase and the topoisomerase IV, essential enzymes for bacterial DNA replication, resulting in bacterial cell death. However, this mechanism can also exert unintended effects on nontargeted cells, such as hMSCs, integral to tissue repair and regeneration. For example, hMSCs exposed to CIP exhibit approximately 50% reduction in proliferation rate compared to cells grown on control substrates without antibiotics [46]. These findings imply that CIP can impair hMSC growth even at sub-lethal concentrations, potentially limiting its application in environments where stem cell proliferation is desired.

The lack of cytotoxic effects in the indirect test indicates that leachable CIP or other coating components do not cause cell death *via* diffusion into the medium. Therefore, the observed reduction in proliferation in the direct assay is not due to soluble toxic components but likely due to the coating's interaction with cells on the surface. The CIP concentration in the surrounding medium is low and does not cause significant cytotoxicity. Therefore, reduced proliferation in the direct contact assay is likely due to the coating's surface properties rather than CIP leaching into the microenvironment. In a recent study, CIP-functionalised bioceramic Ti implants (Ti-HA-CPX) exhibited superior antibacterial activity against *S. aureus* and *E. coli* but showed moderate cytotoxicity on hMSC (70 - 80% cell viability) [50]. Thus, $HACPX_{CS}$ composites, whether chemically synthesised or mechanically mixed ($HACPX_{MM}$), displayed significant cytotoxicity ranging from low to moderate levels. However, CPX can penetrate bone tissue, reach high concentrations and maintain a high drug level at the site of infection, thus eradicating chronic infections and preventing recurrence. CPX from implants is delivered locally, reducing the need for high systemic doses and lowering the risk of systemic toxicity and adverse effects. This feature is significant for patients who may require long-term antibiotic therapy. The authors suggested that Ti-HA-CPX composites are a good option for single-stage surgical interventions in treating chronic osteomyelitis and bone fracture infections. It is worth balancing antibacterial effectiveness with manageable cytotoxicity.

Metabolic activity reduction

The MTS assay results demonstrated a marked reduction in metabolic activity for hMSCs grown on surfaces coated with CIP-loaded materials (*i.e.*, BioHA:LiP-CIP), with activity levels declining by more than 80%. This finding underscores the potent influence of CIP, even at non-cytotoxic concentrations within the coating. The presence of CIP in the BioHA:LiP-CIP coating appeared to impact both cell adhesion and proliferation adversely. This effect is likely attributed to the gradual release of CIP into the surrounding medium, which, despite its antimicrobial efficacy, may inhibit stem cell growth through indirect cytotoxicity or disruption of signalling pathways essential for cell function and proliferation [5]. In addition to its antimicrobial properties, CIP-coated implants have been assessed for biocompatibility [2]. Studies indicate these coatings promote cell viability and bone regeneration without exhibiting significant cytotoxic effects. For example, thin films containing CIP were found to be biocompatible with mouse osteoblast-like cells, suggesting their suitability for biomedical applications [36, 50].

However, while the moderate cytotoxicity has been observed in some formulations, such as those with high concentrations of CIP, these effects can often be managed through careful formulation and coating strategies. The balance between effective antibacterial action and acceptable levels of cytotoxicity is essential for successfully integrating these coatings into clinical practice.

CIP has been shown to influence pathways such as the Wnt/β-catenin pathway, which is crucial for maintaining stemness. Targeting these pathways with specific inhibitors or enhancers could help mitigate adverse effects while harnessing CIP's beneficial aspects.

Research indicates that using nontoxic concentrations of CIP can help maintain stem cell characteristics. For instance, treatment with 10 μg/mL for 72 hours effectively preserved stemness markers in dermal papilla cells (DPCs) while preventing their differentiation into fibroblasts [25]. Another strategy is combining CIP with other agents that may enhance its efficacy while reducing potential harm. For example, studies have shown that mesenchymal stem cells (MSCs) have

antimicrobial properties and can be used alongside antibiotics like CIP to improve outcomes in infection models [53]. This combination could leverage the benefits of both the antibiotic and the regenerative properties of stem cells. Different types of stem cells may respond differently to CIP. Tailoring treatment protocols based on the specific stem cell type can help minimise adverse effects [4].

Further studies are needed to optimise the incorporation of CPX into bioceramic implants to maintain its prolonged antibacterial activity due to sustained release while maintaining acceptable cytotoxicity levels. The capacity of the CPX bioceramic implants to provide a high concentration of antibiotics directly to the site of infection in single-stage surgeries could improve treatment outcomes and decrease healthcare costs associated with prolonged antibiotic therapy and multiple surgeries to benefit the patient.

Conclusions

Integrating CIP into BioHA:LiP coatings have significant implications for achieving antimicrobial efficacy and biocompatibility. While CIP coatings effectively inhibit bacterial viability, the associated reduction in hMSC proliferation and metabolic activity introduces critical considerations for biomaterial applications where cellular compatibility is essential. The study illustrates that direct contact with CIP-coated surfaces negatively impacts stem cell behaviour, whereas indirect exposure does not significantly compromise cell viability, suggesting a nuanced interaction. This dual outcome highlights the need for further research to develop optimised coatings that balance antimicrobial activity and stem cell compatibility. Future studies should aim to refine coating formulations to enhance biocompatibility without compromising antimicrobial efficacy, advancing the development of safer, more effective biomaterials tailored for regenerative medicine applications.

Acknowledgement

The authors acknowledge with thanks the partial financial support of this work by the Romanian Ministry of Research, Innovation, and Digitization under Romanian National Nucleu Program LAPLAS VII–Contract no. 30N/2023. The authors also acknowledge Faik N. Oktar for providing the biological-derived hydroxyapatite powders and I. Negut for her suggestions concerning the FTIR measurements.

Conflict of interest

The authors declare no conflict of interest.

References

1. Abifarin JK, Obada DO, Dauda ET, Dodoo-Arhin D, Experimental data on the characterization of hydroxyapatite synthesized from biowastes. *Data Brief*, 2019; 11(26): 104485.
2. Akshaya S, Rowlo PK, Dukle A, Nathanael AJ, Antibacterial coatings for titanium implants: recent trends and future perspectives. *Antibiotics*, 2022; 11(12): 1719.
3. Arciola CR, Campoccia D, Montanaro L, Implant infections: Adhesion, biofilm formation, and immune evasion. *Nat Rev Microbiol.*, 2018; 16: 397-409.
4. Baltas I, Kavallieros K, Konstantinou G, Koutoumanou E, Gibani MM, Gilchrist M, Davies F, Pavlu J, The effect of CIP prophylaxis during haematopoietic cell transplantation on infection episodes, exposure to treatment antimicrobials and antimicrobial resistance: a single-centre retrospective cohort study. *JAC Antimicrob Resist.*, 2024; 6(1): dlae010.
5. Bonfield TL, Sutton MT, Fletcher DR, Reese-Koc J, Roesch EA, Lazarus HM, Chmiel, JF, Caplan AI, Human mesenchymal stem cell (hMSC) donor potency selection for the "First in Cystic Fibrosis" Phase I Clinical Trial (CEASE-CF). *Pharmaceuticals*, 2023; 16(2): 220.
6. Botterill J, Khatkar H, The role of hydroxyapatite coating in joint replacement surgery – Key considerations. *J Clin Orthop Trauma.*, 2022; 29: 101874.
7. Campion JJ, McNamara PJ, Evans ME, Evolution of CIP-resistant *Staphylococcus aureus* in *in vitro* pharmacokinetic environments. *Antimicrob Agents Chemother.*, 2004; 48(12): 4733-4744.
8. Ciocilteu MV, Mocanu AG, Mocanu A, Ducu C, Nicolaescu OE, Manda VC, Hydroxyapatite-CIP delivery system: Synthesis, characterisation and antibacterial activity. *Acta Pharm.*, 2018; 68(2): 129-144.
9. Ciocilteu MV, Nicolaescu OE, Mocanu AG, Nicolicescu C, Rau G, Neamtu J, Amzoiu E, Amzoiu E, Oancea C, Turcu Stiolica A, Process optimization using quality by design (QBD) approach of a Gentamicin loaded PLGA biocomposite. *Josa*, 2021; 21(4): 1069-1080.
10. Cristescu R, Popescu C, Popescu AC, Grigorescu S, Duta L, Mihailescu IN, Caraene G, Albulescu R, Albulescu L, Andronie A, Stamatin I, Ionescu A, Mihaiescu D, Buruiana T, Chrisey DB, Functionalised polyvinyl alcohol derivatives thin films for controlled drug release and targeting systems: MAPLE deposition and morphological, chemical and *in vitro* characterization. *Appl Surf Sci.*, 2009; 255(10): 5600-5604.
11. Cristescu R, Popescu C, Popescu AC, Grigorescu S, Duta L, Mihailescu IN, Andronie A, Stamatin I, Ionescu OS, Mihaiescu D, Buruiana T, Chrisey DB, Laser processing of polyethylene glycol derivative and block copolymer thin films. *Appl Surf Sci.*, 2009; 255(10): 5605-5610.
12. Dinda GP, Shin J, Mazumder J, Pulsed laser deposition of hydroxyapatite thin films on Ti–6Al–4V: effect of heat treatment on structure and properties. *Acta Biomater.*, 2009; 5(5): 1821-1830.
13. Dorcioman G, Grumezescu V, Stan GE, Chifiriuc MC, Gradisteanu GP, Miculescu F, Matei E, Popescu-Pelin G, Zgura I, Craciun V, Oktar FN, Duta L, Hydroxyapatite Thin Films of Marine Origin as Sustainable Candidates for Dental Implants. *Pharmaceutics*, 2023; 15(4): 1294.

14. Duta L, Popescu AC, Current status on pulsed laser deposition of coatings from animal-origin calcium phosphate sources. *Coatings*, 2019; 9(5): 335.
15. Duta L, Ristoscu C, Stan GE, Husanu MA, Besleaga C, Chifiriuc MC, Lazar V, Bleotu C, Miculescu F, Mihailescu N, Axente E, Badiceanu M, Bociaga D, Mihailescu IN, New bio-active, antimicrobial and adherent coatings of nanostructured carbon double-reinforced with silver and silicon by Matrix-Assisted Pulsed Laser Evaporation for medical applications. *Appl Surf Sci.*, 2018; 441: 871-883.
16. Duta L, Stan GE, Popescu-Pelin G, Zgura I, Anastasescu M, Oktar FN, Influence of post-deposition thermal treatments on the morpho-structural, and bonding strength characteristics of lithium-doped biological-derived hydroxyapatite. *Coatings*, 2022; 12(12): 1883.
17. Duta L, Oktar FN, Stan GE, Popescu Pelin G, Serban N, Luculescu A, Mihailescu IN, Novel doped hydroxyapatite thin films obtained by pulsed laser deposition. *Appl Surf Sci.*, 2013; 265: 41-49.
18. Florian PE, Duta L, Grumezescu V, Popescu-Pelin G, Popescu AC, Oktar FN, Evans RW, Constantinescu AR, Lithium-doped biological-derived hydroxyapatite coatings sustain *in vitro* differentiation of human primary mesenchymal stem cells to osteoblasts. *Coatings*, 2019; 9(12): 781.
19. Firsov AA, Vostrov SN, Shevchenko AA, Zinner SH, Cornaglia G, Portnoy YA, MIC-based interspecies prediction of the antimicrobial effects of CIP on bacteria of different susceptibilities in an *in vitro* dynamic model. *Antimicrob Agents Chemother.*, 1998; 42(11): 2848-2852.
20. Gill LR, Mayberry-Carson KJ, Tober-Meyer B, Hodin F, Lambe DW Jr, Painter BG, CIP concentrations in serum, bone and bone marrow of rabbits. *Microbios.*, 1989; 58(235): 113-126.
21. Grant-Jacob JA, Beecher SJ, Prentice JJ, Shepherd DP, Mackenzie JI, Eason RW, Pulsed laser deposition of crystalline garnet wave guides at a growth rate of 20 μm *per* hour. *Surf Coat Technol.*, 2018; 343: 7-10.
22. Homa K, Zakrzewski W, Dobrzyński W, Piszko PJ, Piszko A, Matys J, Wiglusz RJ, Dobrzyński M, Surface functionalization of titanium-based implants with a nanohydroxyapatite layer and its impact on osteoblasts: a systematic review. *J Funct Biomater.*, 2024; 15(2): 45.
23. Ionescu C, Rizea SC, Pîrvu A, Vlase L, Barragan-Montero V, Neamțu J, Synthesis of an amphiphilic compound derived from malonic acid for bone targeting. *Farmacia*, 2022; 70(1): 59-64.
24. Janković A, Eraković S, Ristoscu C, Mihailescu Serban N, Duta L, Visan A, Stan GE, Popa AC, Husanu MA, Luculescu CR, Srdić VV, Janaćković Dj, Mišković-Stanković V, Bleotu C, Chifiriuc MC, Mihailescu IN, Structural and biological evaluation of lignin addition to simple and silver-doped hydroxyapatite thin films synthesized by matrix-assisted pulsed laser evaporation. *J Mater Sci Mater Med.*, 2015; 26(1): 5333.
25. Kiratipaiboon C, Tengamnuay P, Chanvorachote P, CIP improves the stemness of human dermal papilla cells. *Stem Cells Int.*, 2015; 2016: 5831276.
26. Kunisada T, Nakata E, Fujiwara T, Hata T, Sato K, Katayama H, Kondo A, Ozaki T, Clinical application of unidirectional porous hydroxyapatite to bone tumour surgery and other orthopaedic surgery. *Biomimetics*, 2024; 9(5): 294.
27. Kowalczuk D, Gładysz A, Pitucha M, Kamiński DsM, Barańska A, Drop B, Spectroscopic study of the molecular structure of the new hybrid with a potential two-way antibacterial effect. *Molecules*, 2021; 26(5): 1442.
28. Kylychbekov S, Allamyradov Y, Khuzhakulov Z, Majidov I, Banga S, ben Yosef J, Duta L, Er AO, Bioactivity and mechanical properties of hydroxyapatite on Ti6Al4V and Si (100) surfaces by pulsed laser deposition. *Coatings*, 2023; 13(10): 1681.
29. Luo, J, Mamat B, Yue Z, Zhang N, Xu X, Li Y, Su Z, Ma C, Zang F, Wang Y, Multi-metal ions doped hydroxyapatite coatings *via* electrochemical methods for antibacterial and osteogenesis. *Colloid Interface Sci Commun.*, 2021; 43: 100435.
30. May-Smith TC, Muir AC, Darby MSB, Eason RW, Design and performance of a ZnSe tetra-prism for homogeneous substrate heating using a CO_2 laser for pulsed laser deposition experiments. *Applied Optics.*, 2008; 47(11): 1767-1780.
31. Mihailescu N, Stan GE, Duta L, Chifiriuc MC, Bleotu C, Sopronyi M, Luculescu C, Oktar FN, Mihailescu IN, Structural, compositional, mechanical characterization and biological assessment of bovine-derived hydroxyapatite coatings reinforced with MgF_2 or MgO for implants functionalization. *Mat Sci Eng C.*, 2016; 59: 1-6.
32. Mîndrilă I, Osman A, Mîndrilă B, Predoi MC, Mihaiescu DE, Buteică SA, Phenotypic switching of B16F10 melanoma cells as a stress adaptation response to Fe_3O_4/salicylic acid nanoparticle therapy. *The Pharmaceuticals*, 2021; 14(10): 1007.
33. Nair SP, Meghji S, Wilson M, Reddi K, White P, Henderson B, Bacterially induced bone destruction: mechanisms and misconceptions. *Infect Immun.*, 1996; 64(7): 2371-2380.
34. Neamtu J, Bubulică MV, Rotaru A, Ducu C, Balosache OE, Manda VC, Turcu-Stiolica A, Nicolicescu C, Melinte R, Popescu M, Croitoru O, Hydroxyapatite-alendronate composite systems for biocompatible materials. *J Therm Anal Calorim.*, 2017; 127: 1567-1582.
35. Negroiu G, Piticescu RM, Chitanu GC, Mihailescu IN, Zdrentu L, Miroiu M, Biocompatibility evaluation of a novel hydroxyapatite- polymer coating for medical implants (*in vitro* tests). *J Mater Sci.*, 2008; 19: 1537-1544.
36. Negut I, Ristoscu C, Tozar T, Dinu M, Parau AC, Grumezescu V, Hapenciuc C, Popa M, Stan MS, Marutescu L, Mihailescu IN, Chifiriuc MC, Implant surfaces containing bioglasses and CIP as platforms for bone repair and improved resistance to microbial colonization. *Pharmaceutics*, 2022; 14(6): 1175.
37. Neyestani Z, Khademi F, Teimourpour R, Prevalence and mechanisms of CIP resistance in *Escherichia coli* isolated from hospitalised patients, healthy carriers and wastewaters in Iran. *BMC Microbiol.*, 2023; 23: 191.
38. Nichol T, Callaghan J, Townsend R, Stockley I, Hatton PV, Le Maitre C, Smith TJ, Akid R, The antimicrobial activity and biocompatibility of a controlled gentamicin-releasing single-layer sol-gel coating on hydroxyapatite-coated Titanium. *Bone Joint J.*, 2021; 103-B: 522-529.
39. Overbeck JP, Winckler ST, Meffert R, Törmälä P, Spiegel HU, Brug E, Penetration of CIP into bone: a

new bioabsorbable implant. *J Invest Surg.*, 1995; 8(3): 155-162.
40. Oktar FN, Unal S, Gunduz O, Nissan BB, Macha IJ, Akyol S, Duta L, Ekren N, Altan E, Yetmez M, Marine-derived bioceramics for orthopaedic, reconstructive and dental surgery applications. *J Aust Ceram Soc.*, 2022; 59(1): 1-25.
41. Pandey S, Pandey P, Tiwari G, Tiwari R, Rai AK, FTIR spectroscopy: a tool for quantitative analysis of CIP in tablets. *Indian J Pharm Sci.*, 2012; 74(1): 86-90.
42. Predoi MC, Mîndrilă I, Buteică SA, Purcaru ȘO, Mihaiescu DE, Mărginean OM, Iron oxide/salicylic acid nanoparticles as potential therapy for B16F10 melanoma transplanted on the chick chorioallantoic membrane. *Processes*, 2020; 8(6): 706.
43. Popescu AC, Florian PE, Stan GE, Popescu-Pelin G, Zgura I, Enculescu M, Oktar FN, Trusca R, Sima LE, Roseanu A, Duta L, Physical-chemical characterization and biological assessment of simple and lithium-doped biological-derived hydroxyapatite thin films for a new generation of metallic implants. *Appl Surf Sci.*, 2018; 439: 724-735.
44. Rashidian Vaziri MR, Hajiesmaeilbaigi F, Maleki MH, Monte Carlo simulation of the subsurface growth mode during pulsed laser deposition. *J Appl Phys.*, 2011; 110 (4): 043304.
45. Sima LE, Stan GE, Morosanu CO, Melinescu A, Ianculescu A, Melinte R, Neamtu J, Petrescu SM, Differentiation of mesenchymal stem cells onto highly adherent radio frequency-sputtered carbonated hydroxyl-apatite thin films. *J Biomed Mater Res A.*, 2010; 95(4): 1203-1214.
46. Sisto F, Bonomi A, Cavicchini L, Coccè V, Scaltrito MM, Bondiolotti G, Alessandri G, Parati E, Pessina A, Human mesenchymal stromal cells can uptake and release CIP, acquiring *in vitro* anti-bacterial activity. *Cytother.*, 2014; 16(2): 181-190.
47. Souza JCM, Sordi MB, Kanazawa M, Ravindran S, Henriques B, Silva FS, Aparicio C, Cooper LF, Nano-scale modification of titanium implant surfaces to enhance osseointegration. *Acta Biomater.*, 2019; 94: 112-131.
48. Surmenev RA, A review of plasma assisted methods for calcium phosphate-based coatings fabrication. *Surf Coat Technol.*, 2012; 206: 2035-2056.
49. Turcu Stiolica A, Bubulica MV, Nicolaescu OE, Croitoru O, Popescu M, Manda VC, Simionescu A, Neamtu J, A design of experiment approach to the synthesis of alendronate-incorporated hydroxyapatite. *Rev Chim.*, 2018; 69(8): 1944-1948.
50. Văruț RM, Rotaru LT, Cimpoesu D, Corlade M, Singer CE, Popescu AIS, Popescu C, Iliescu IN, Mocanu A, Popescu M, Butoi MA, Nicolaescu OE, Enhanced antibacterial efficacy of bioceramic implants functionalised with CIP: an *in silico* and *in vitro* study. *Pharmaceutics*, 2024; 16(8): 998.
51. Visan A, Grossin D, Stefan N, Duta L, Miroiu FM, Stan GE, Sopronyi M, Luculescu C, Freche M, Marsan O, Charvillat C, Ciuca S, Mihailescu IN, Biomimetic nanocrystalline apatite coatings synthesized by Matrix Assisted Pulsed Laser Evaporation for medical applications. *Mat Sci Eng B.*, 2014; 181: 56-63.
52. Wu H, Chen X, Kong L, Liu P, Mechanical and biological properties of titanium and its alloys for oral implant with preparation techniques: a review. *Materials*, 2023; 16(21): 6860.
53. Yoshitani J, Kabata T, Arakawa H, Kato Y, Nojima T, Hayashi K, Tokoro M, Sugimoto N, Kajino Y, Inoue D, Ueoka K, Yamamuro Y, Tsuchiya H, Combinational therapy with antibiotics and antibiotic-loaded adipose-derived stem cells reduce abscess formation in implant-related infection in rats. *Sci Rep.*, 2020; 10(1): 11182.